Journal of Porphyrins and Phthalocyanines
J. Porphyrins Phthalocyanines 2017; **21**: 1–10
DOI: 10.1142/S1088424617500365
Published at http://www.worldscinet.com/jpp/

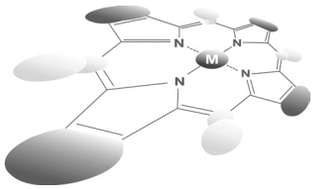

Metal-porphyrin catalyzed aziridination of α-methylstyrene: Batch *vs.* flow process

Daniela Intrieri*, Sergio Rossi*, Alessandra Puglisi and Emma Gallo

Dipartimento di Chimica, Università Degli Studi di Milano, Via Camillo Golgi 19, 20133 Milano, Italy

Dedicated to Professor Claudio Ercolani on the occasion of his 80th birthday

Received 20 January 2017
Accepted 16 March 2017

ABSTRACT: This work describes the aziridination process of α-methylstyrene by using electron poor aromatic azides in the presence of metal-based porphyrins as catalysts. Different ruthenium and cobalt-based porphyrins were successfully employed for the synthesis of *N*-aryl aziridines performed under a traditional batch methodology and under continuous flow conditions. In general, yields obtained using ruthenium-based catalysts in a traditional batch process were higher than those observed when the reaction was performed under flow conditions. However, cobalt-based porphyrins showed better activities and short reaction times when employed in a flow system process. DFT calculations were also performed in order to understand the influence of substituents on the porphyrin ring in the aziridination process.

KEYWORDS: homogeneous catalysis, ruthenium, cobalt, aziridination, azide, flow chemistry.

INTRODUCTION

Considering the biological and/or pharmaceutical importance of nitrogen containing molecules, the scientific community is always interested in developing new synthetic methodologies to obtain them in good yields and selectivities [1]. Among all reagents employed for the synthesis of aza-derivatives, aziridines are extensively used as building block in organic synthesis thanks to the high reactivity of the strained three-membered rings, which can easily be involved in ring opening reactions [2–7]. Among all the synthetic available procedures yielding aziridines, the metal-catalyzed nitrene transfer reaction to unsaturated hydrocarbons represents a valuable strategy to obtain this class of compounds [8–10].

The use of imidoiodinane compounds (R′I = NR) as nitrogen sources have been extensively studied [11–15], but several drawbacks related to their use encouraged scientists to investigate the reactivity of alternative starting materials in order to optimize the reaction efficiency. Following on, organic azides (RN_3) represent a versatile class of reactants which are very reactive toward different substrates and are easily synthesized from commercially available amines [16–19]. Moreover, they generate the nitrene moiety (RN) with the contemporary formation of benign N_2 as the only stoichiometric by-product (Scheme 1).

The use of organic azides as starting materials have been restricted due to their hazardous nature, thus more stable compounds were preferred. However more recent continuous flow methodologies are being applied to minimize this limitation [20]. This approach provides safe handling of hazardous reagents by using small amounts of chemicals with a consequent decrease of the process risks and a shortness of reaction times.

We recently reported the use of continuous flow methodologies for the aziridination of styrenes by using aromatic azides as nitrene sources and Ru(TPP)CO (TPP = dianion of tetraphenyl porphyrin) as the reaction catalyst [21, 22]. In order to expand our recent study of the catalytic reaction of aryl azides with styrenes affording *N*-aryl aziridines, we focused our attention on the use of different metal-based porphyrins by

*Correspondence to: Daniela Intrieri, email: daniela.intrieri@unimi.it; Sergio Rossi, email: sergio.rossi@unimi.it, tel: +39 025-031-4371

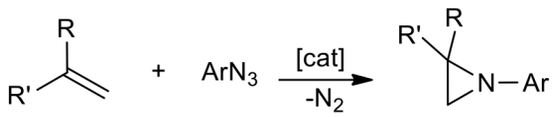

Scheme 1. General route for the aziridinations of alkenes by organic azides

applying continuous flow techniques. With this purpose, we systematically investigated how electronic and/or steric features of porphyrin complexes influence their catalytic activity. Herein we report the use of different metal porphyrins in promoting aziridination reactions in flow conditions as well as the comparison of achieved data with those obtained working in batch conditions. In addition, achieved experimental results were supported by a DFT investigation of reported catalytic reactions.

RESULTS AND DISCUSSION

In order to study the electronic and steric influence of porphyrin ligands on the catalytic activity of ruthenium and cobalt complexes, we tested different catalysts **3a–3i** listed in Scheme 2 in the aziridination of α-methylstyrene (**1**), by using either 3,5-*bis*(trifluoromethyl)phenyl azide (**2a**) or 4-nitrophenyl azide (**2b**) as the aminating agent.

Ruthenium porphyrin complexes [23–25] **3a–3f** efficiently promoted the synthesis of both aziridines **4a** and **4b** in batch conditions (Table 1). The synthesis of **4a** occurred with slightly lower yields than those already achieved for **4b** [23], however a decrease in reaction times was generally observed. As reported in Table 1, the efficiency of the synthesis of **4a** did not strongly depend on electronic and steric characteristics of the porphyrin catalyst. The desired aziridine **4a** was formed in 94% yield (Table 1, entry 1) in the presence of Ru(TPP)CO (**3a**), which presents unsubstituted *meso*-phenyl groups and only small differences of the catalytic efficiency were observed by using ruthenium porphyrin catalysts showing differently substituted *meso*-aryl groups. The lowest yield was registered in the presence of catalyst **3d** (Table 1, entry 7) where steric effects became more evident due to the presence of two CF_3 groups on *meta* positions of *meso*-aryl groups.

Cobalt porphyrin complexes **3g–3i** demonstrated to be less catalytically active in batch conditions (Table 2) than ruthenium complexes and longer reaction times and lower yields were generally observed.

A better catalytic performance was usually observed for the synthesis of aziridine **4a** independently from the electronic and steric nature of the porphyrin ligand. On the other hand, low yields registered in the synthesis of **4b** were probably due to the lower chemical stability of 3,5-*bis*(trifluoromethyl)phenyl azide **2a** in refluxing benzene when the catalytic reaction was run for a long time to reach complete azide conversion.

In order to improve the efficiency of **4a** and **4b** synthesis catalyzed by ruthenium and cobalt porphyrin-complexes, we performed reactions described above under flow conditions. We realized a simple 500 μL microreactor using a PolyTetraFluoroEthylene (PTFE) HPLC tubing (see the Supporting information section for further details). The flow apparatus was settled up as illustrated in Scheme 3, and the reactions were performed under previously identified standard conditions [21]. A Chemix Fusion syringe pump equipped with two 2.5 mL Hamilton gastight syringes was used to feed the microreactor with the reagents through a T-junction (Syringe A: 0.008 M solution of catalyst in α-methylstyrene as the solvent; Syringe B: 0.4 M azide solution in α-methylstyrene as the solvent, biphenyl as the internal standard). The microreactor was coiled in a bundle and immersed in a

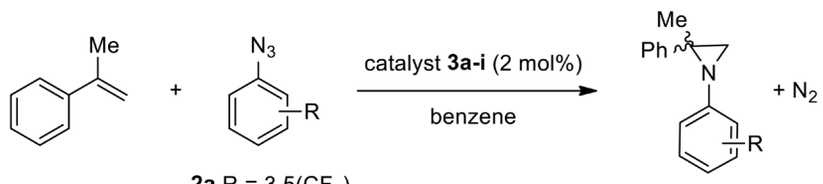

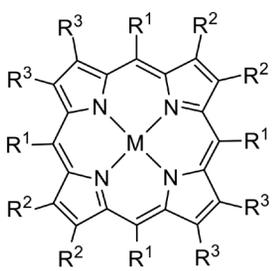

3a, Ru(TPP)CO: M=Ru(CO), R^1=C_6H_5, R^2=R^3=H
3b, Ru(OEP)CO: M=Ru(CO), R^1=H, R^2=R^3=C_2H_5
3c, Ru(β-Br_4TPP)CO: M=Ru(CO), R^1=C_6H_5, R^2=Br, R^3=H
3d, Ru(3,5$(CF_3)_2$TPP)CO: M=Ru(CO), R^1=3,5$(CF_3)_2C_6H_3$, R^2=R^3=H
3e, Ru(4^{n}BuTPP)CO: M=Ru(CO), R^1=4(^{n}Bu)C_6H_4, R^2=R^3=H
3f, Ru(TMP)CO: M=Ru(CO), R^1=2,4,6$(CH_3)_3C_6H_2$, R^2=R^3=H
3g, Co(OEP): M=Co, R^1=H, R^2=R^3 =C_2H_5
3h, Co(TPP): M=Co, R^1=C_6H_5, R^2=R^3=H
3i, Co(TMOP): M=Co, R^1=4$(CH_3O)C_6H_4$, R^2=R^3=H

Scheme 2. Complexes **3a**–**3i**-catalyzed aziridination of α-methylstyrene by either 3,5-*bis*(trifluoromethyl)phenyl azide (**2a**) or 4-nitrophenyl azide (**2b**)

Table 1. [a]In a typical run, the opportune catalyst (1.20×10^{-5} mol) the opportune azide (6.00×10^{-4} mol) and α-methylstyrene (2.50×10^{-3} mol) were added to benzene (25 mL) in a Schlenk flask. [b]Time required for complete conversion of the starting azide monitored by IR spectroscopy. [c]Determined by ^{1}H NMR employing 2,4-dinitrotoluene as the internal standard

Entry[a]	Catalyst	Time, h[b]	Yield, %[c]	
1	Ru(TPP)CO (**3a**)	0.5	**4a**	94
2		0.75	**4b**	99
3	Ru(OEP)CO (**3b**)	0.5	**4a**	94
4		1.5	**4b**	96
5	Ru(β-Br_4TPP)CO (**3c**)	0.5	**4a**	86
6		0.5	**4b**	98
7	Ru(3,5(CF_3)$_2$TPP)CO (**3d**)	0.5	**4a**	78
8		1	**4b**	98
9	Ru(4*n*BuTPP)CO (**3e**)	0.5	**4a**	88
10		1	**4b**	99
11	Ru(TMP)CO (**3f**)	0.5	**4a**	92
12		2	**4b**	95

Table 2. [a]In a typical run, the opportune catalyst (1.20×10^{-5} mol) the opportune azide (6.00×10^{-4} mol) and α-methylstyrene (2.50×10^{-3} mol) were added to benzene (25 mL) in a Schlenk flask. [b]Time required for complete conversion of the starting azide monitored by IR spectroscopy. [c] Determined by ^{1}H NMR employing 2,4-dinitrotoluene as internal standard

Entry[a]	Catalyst	Time, h[b]	Yield, %[c]	
1	Co(OEP) (**3g**)	1	**4a**	51
		8	**4b**	46
2	Co(TPP) (**3h**)	3.5	**4a**	56
		16	**4b**	4
3	Co(TMOP) (**3i**)	4	**4a**	41
		15	**4b**	10

120 °C preheated oil bath. Conversion was determined by GC analysis of the crude mixture collected after 30 min at -30 °C. Results are reported in Table 3.

Aziridine **4a** was obtained in high yields when either Ru(TPP)CO (**3a**) or Ru(OEP)CO (**3b**) (OEP = dianion of octaethyl porphyrin) were employed as catalysts (Table 3, entries 1–2) whilst, as expected, lower yields where observed when less active azide **2b** was employed as the starting material. These data are in agreement with those obtained in batch condition, where compound **2b** required longer reaction time in order to form product **4b** in a quantitative yield (Table 1, entries 1–2).

The use of sterically hindered catalyts such as Ru(β-Br_4TPP)CO (**3c**) (β-Br_4TPP = dianion of 2,3,12,13-tetrabromo-tetraphenylporphyrin) or Ru(3,5(CF_3)$_2$TPP)CO (**3d**) (3,5(CF_3)$_2$TPP = dianion of tetrakis(3,5-*bis*(trifluoromethyl)phenyl)porphyrin), bearing electron withdrawing groups on the porphyrin ring, caused a decrease in yields and product **4a** was obtained with 67% and 49% yield, respectively. A small decrease in terms of yields was also observed when the more electron rich ruthenium porphyrin catalyst **3e** was used, leading to the formation of the desired product with 82% yield (Table 3, entry 5). This negative catalytic effect was also observed when a xylene residue was present on the *meso*-position of catalyst **3f** and aziridine **4a** was obtained in only 69% yield (Table 3, entry 7).

A general lower reactivity was observed when 4-nitrophenyl azide (**2b**) was employed in the aziridination of α-methylstyrene performed under continuous flow conditions, where only catalysts Ru(TPP)CO (**3a**) and Ru(OEP)CO (**3b**) led to the formation of corresponding product **4a** in good yields (Table 3, entries 1–2). Catalyst Ru(β-Br_4TPP)CO (**3c**) afforded the desired product with 48% yield, but the most electron poor catalyst Ru(3,5(CF_3)$_2$TPP)CO (**3d**) seemed not to be effective in the reaction involving 4-nitrophenyl azide (**2b**) (Table 3, entry 4). However, clear evidence of these results showed that only Ru(TPP)CO (**3a**) and Ru(OEP)CO (**3b**) catalysts were able to preserve their catalytic efficiency when employed under flow conditions.

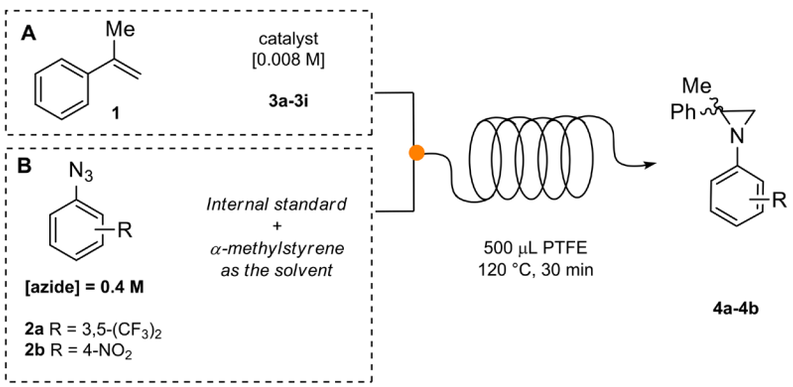

Scheme 3. Reaction between azides **2a–2b** and α-methylstyrene **1** promoted by ruthenium and cobalt porphyrin complexes in a two-syringe continuous-flow system by using a 500 µL mesoreactor

Table 3. [a] In a typical run, A and B mixtures were fed into the 120 °C pre-heated 500 µL PTFE mesoreactor using a syringe pump (flow rate 8.333 µL/min; residence time 30 min). Mixture A: catalyst (1.60×10^{-5} mol) in 2 mL of **1**. Mixture B: azide (8.00×10^{-4} mol), biphenyl as the internal standard (6.00×10^{-5} mol) in 2 mL of **1**. [b] Determined by GC employing biphenyl as the internal standard

Entry[a]	Catalyst		Product **4a** GC yield, %[b]	Product **4b** GC yield, %[b]
1	Ru(TPP)CO	**3a**	98	64
2	Ru(OEP)CO	**3b**	97	70
3	Ru(β-Br_4TPP)CO	**3c**	67	48
4	Ru(3,5(CF_3)$_2$TPP)CO	**3d**	49	14
5	Ru(4^{n}Bu-TPP)CO	**3e**	82	38
6	Ru(TMP)CO	**3f**	69	21

Table 4. [a] In a typical run, A and B mixtures were fed into the 120 °C pre-heated 500 µL PTFE mesoreactor using a syringe pump (flow rate = 8.333 µL/min; residence time = 30 min). Mixture A: catalyst (1.60×10^{-5} mol) in 2 mL of **1**. Mixture B: azide (8.00×10^{-4} mol), biphenyl as the internal standard (6.00×10^{-5} mol) in 2 mL of **1**. [b] Determined by GC employing biphenyl as the internal standard

Entry[a]	Catalyst		Product **4a** GC yield, %[b]	Product **4b** GC yield, %[b]
1	Co(OEP)	**3g**	69	52
2	Co(TPP)	**3h**	66	48
3	Co(TMOP)	**3i**	73	36

In order to improve the catalytic performance of the aziridination of α-methylstyrene under flow conditions, we then moved to the investigation of the catalytic activity of cobalt porphyrin catalysts **3g**–**3i**. Results are reported in Table 4.

We were delighted to see that the use of cobalt-base porphyrin catalysts for the aziridination of α-methylstyrene under mesofluidic conditions presented a beneficial effect in terms of yields, especially if compared with their activity which was observed using the traditional batch approach (Table 4 *vs.* Table 2). Best results were obtained with catalyst Co(TMOP) (**3i**) (TMOP = dianion of tetrakis(4-methoxyphenyl) porphyrin) that afforded product **4a** in 73% yield after 30 min of residence time. Even better results were achieved with catalysts Co(OEP) (**3g**) and Co(TPP) (**3h**), affording product **4a** in comparable yields. Furthermore, with this approach, 4-nitrophenyl azide (**2b**) also was found to be reactive in the synthesis of aziridine **4b**. It can be noted that, in the presence of catalyst Co(OEP) (**3g**) under traditional batch conditions, only traces of product were isolated after 16 h (Table 2, entry 3) which increased up to 48% yield by means of the flow approach (with 30 min of residence time). As a general consideration, better results in terms of yields were also obtained with other cobalt-based porphyrin catalysts.

Furthermore, the possibility to operate under flow conditions presents the advantage of operating with smaller reaction volumes and in the absence of solvent.

DFT CALCULATIONS

Theoretical studies were also performed in order to understand the influence of substituents on the porphyrin ring in the aziridination process and to elucidate the differences in terms of the energy barrier profile using different ruthenium porphyrin complexes. Since it was already established that ruthenium and cobalt-based aziridinations occur through different mechanisms [26, 27], the two catalytic reactions were not compared and the cobalt-catalyzed aziridination was not the object of this DFT investigation. The overall energy profile for the aziridination of α-methylstyrene (**1**) with 3,5-*bis*(trifluoromethyl)phenyl azide (**2a**) catalyzed by ruthenium porphyrin complexes was already investigated [28] by means of kinetic studies and DFT calculations. A general overview of the mechanism is reported in Scheme 4. It is known that the first step of the mechanism involves the coordination of the azide to ruthenium complex **A** to form **B**. This coordination results in the activation of the azide ArN_3 and the consequent eco-friendly dismissal of a neutral N_2 molecule leading to the formation of the diradical *mono*-imido [Ru](NAr)(CO) complex **C** ([Ru] = ruthenium porphyrin) which, depending on the reaction conditions, can be involved in a singlet → triplet spin crossing process. Complex **C(t)**, in its triplet state can react with the incoming olefin and transfer one of the nitrogen unpaired electrons to the distal olefin carbon atom forming the metastable and diradical N–C–C open chain complex **D**. Consequent minor

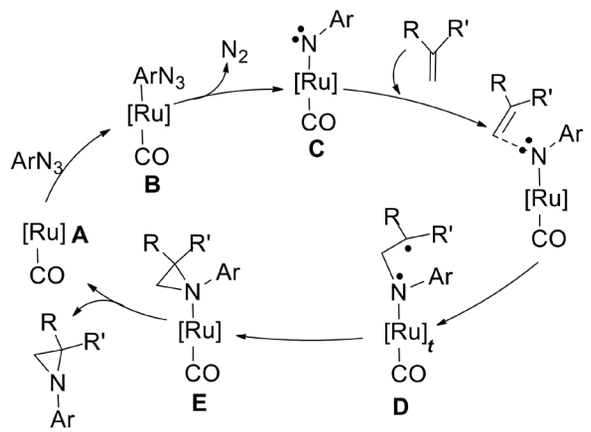

Scheme 4. Overall mechanism of the [Ru](CO)-catalyzed aziridination of α-methylstyrene by ArN_3

stereochemical rearrangements of this latter compound are finally responsible for the aziridine ring closure by a spin coupling process. After the release of the aziridine product from **E**, the initial ruthenium porphyrin complex **A** is restored and available for a new catalytic cycle.

Considering that previous work established that the high-demanding energy step (formally, the Rate-Determining Step) involves the release of N_2 molecule [28, 29], we focused our attention in determining the energy barrier of this step related to all the different ruthenium porphyrins **3a**–**3f** employed in this study.

Firstly, a conformational analysis with Monte Carlo techniques, performed with OPLS_2005 force field [30] on a simple model of all the structures analyzed below, achieves the best conformation of differently substituted porphyrin molecules (the ruthenium atom was replaced with a generic octahedral six-coordinated atom for simplicity of calculations). Subsequently, all the optimized structures were validated as minima or transition states by DFT calculations (after the replacement of the generic atom with the ruthenium atom) where the optimization and calculation of the thermochemical properties were performed with B97D functional [31], the effective Stuttgart/Dresden core potential (SDD) was adopted for the ruthenium atom and for all the other atomic species the basis set applied was 6-31G(d). All the calculations were performed *in vacuum* by using Gaussian G09 rev D01 package [32]. The calculated energy profiles for the generation of *mono*-imido complexes **Ca–Cf** are shown in Fig. 1, energies values are reported in Table 5 and the coordinates of all the optimized structures are described in the Supplementary material (see the Supporting information section).

As expected, the anchoring step of the N_α azide atom of **2a** to the metal center of the porphyrin was a favorite process [28, 29] and a high stabilization was observed when catalysts **3c** and **3f** (-4.20 kcal/mol and -4.15 kcal/mol, respectively) were used. Interestingly, the performed calculations showed that in all the cases investigated, the energy barrier required for the generation of *mono*-imido

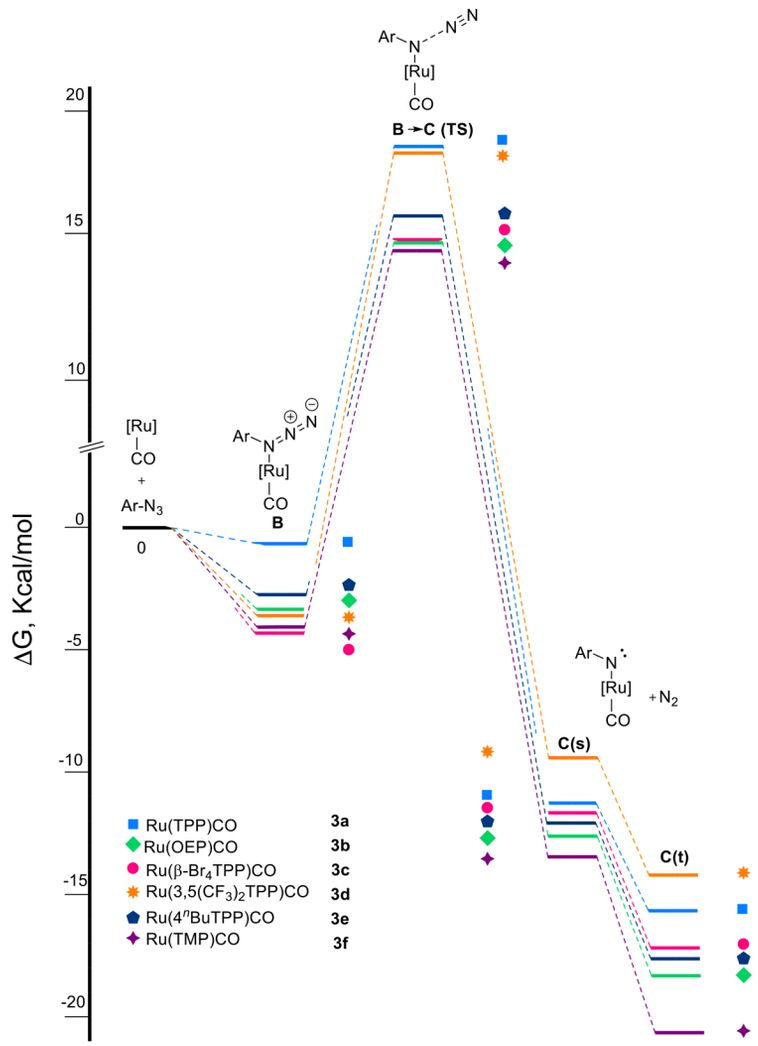

Fig. 1. Energy profile for the generation of *mono*-imido complexes **Ca–Cf**

Table 5. Free energy values calculated at the B97D/6-31G(d) Ru(SDD) level of theory. All the transition states presented one imaginary frequency.

Catalyst		Complex **B** ΔG°, kcal/mol[a]	**B → C (TS)** ΔG#, kcal/mol[b]	**B → C barrier, kcal/mol[c]**	Complex **C(s)** ΔG°, kcal/mol [a]	Complex **C(t)** ΔG°, kcal/mol [a]	**ΔΔG°$_{C(s)\rightarrow(t)}$**, kcal/mol[d]
Ru(TPP)CO	**3a**	-1.53	18.57	**20.10**	-11.22	-15.63	**-4.41**
Ru(OEP)CO	**3b**	-3.40	14.82	**18.22**	-12.64	-18.70	**-6.06**
Ru(β-Br$_4$TPP)CO	**3c**	-4.20	14.83	**19.03**	-11.48	-17.16	**-5.68**
Ru(3,5(CF$_3$)$_2$TPP)CO	**3d**	-3.47	18.41	**21.87**	-9.39	-14.15	**-4.76**
Ru(4^{n}Bu-TPP)CO	**3e**	-2.86	15.85	**18.71**	-12.20	-17.51	**-5.31**
Ru(TMP)CO	**3f**	-4.15	14.27	**18.43**	-13.17	-20.79	**-7.62**

[a] ΔG° values represent the standard free energy of the corresponding ground state. [b] ΔG# values represent the standard free energy of the corresponding transition state. [c] The energy barrier was calculated as ΔG#–ΔG°. [d] Calculated as ΔG°$_{C(t)}$–ΔG°$_{C(s)}$.

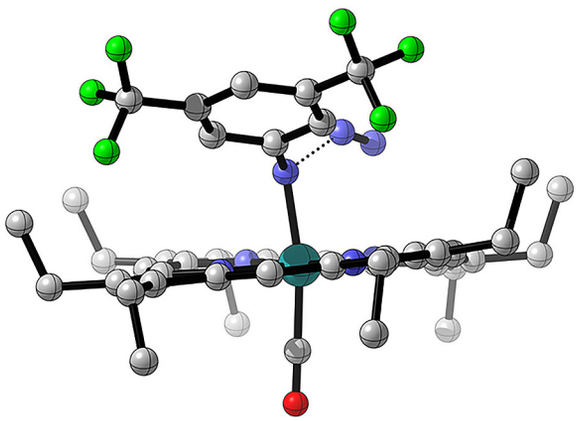

Fig. 2. Transition state structure related to the interaction of catalyst **3f** with azide **2a**. Hydrogen atoms were omitted for clarity

complexes **C(s)** was about 20 kcal/mol, in accordance with that already reported by some of us and consistent with the high temperature required for the catalysis to proceed [28, 29].

Catalyst Ru(OEP)CO (**3b**) presented the lowest energy barrier (18.22 kcal/mol) probably due to the absence of steric interactions between the aromatic ring of the 3,5-*bis*(trifluoromethyl)phenyl azide (**2a**) and the hydrogen atoms on the *meso*-positions of the porphyrin moiety. As showed in Fig. 2, the azide molecule was perfectly hosted between the ethyl substituents of the catalyst, the CF_3 groups of the azide and the terminal CH_3 groups of the ethyl substituents on β-pyrrolic porphyrin positions adopted an *anti* conformation, where the shortest distance H_{porp}••••F_{azide} was about 2.6 A. This situation was observed only when a β-substituted catalyst interacts with the azide reactant.

Catalysts Ru(4^{n}BuTPP)CO (**3e**) (4^{n}BuTPP = dianion of tetrakis(4-*n*-butylphenyl)porphyrin) and Ru(TMP)CO (**3f**) (TMP = dianion of tetramesityl porphyrin) presented a comparable lower energy barrier (18.71 kcal/mol and 18.43 kcal/mol respectively) meaning that the presence of electron donating substituents on the porphyrin ring played a positive effect on the chemical efficiency of the process, as confirmed by high aziridine **4a** yields observed in the presence of these catalysts by applying traditional batch conditions (Table 1, entries 9 and 11). The presence of electron withdrawing substituents, such as the four bromine atoms of catalyst Ru(β-Br$_4$TPP)CO (**3c**), seemed to have a minor influence on the interaction of azide **2a** with the ruthenium complex, probably because the distortion induced by substituents on the porphyrin ring caused a less steric hindrance between the porphyrin and the aromatic ring of the incoming azide. However, the lower electron density present on the ruthenium atom of the catalyst induces a small decrease of reaction yields (Table 3, entry 3).

Surprising, Ru(TPP)CO (**3a**) presents an energy barrier of 20.10 kcal/mol, that was +1.39 kcal/mol higher than that calculated when the electron rich Ru(4^{n}BuTPP)CO (**3e**) was applied as the reaction catalyst. This could be explained considering possible π-staking interactions between hydrogen atoms of the porphyrin phenyl substituents and the aromatic ring of the azide. The analysis of the geometry of **3a** and **3e** transition states revealed that only in the case of **3e**, hydrogen atoms in the *ortho* position of the phenyl ring were oriented toward the aromatic ring of the azide with a consequent stabilization of the interaction. On the other hand, the absence of any stabilization process in the interaction of **3a** with azide **2a** explains the observed increase of the energy barrier when **3a** was applied (Fig. 3).

The presence/absence of this kind of interaction was confirmed by performing a non-covalent interaction (NCI) analysis, using NCIPLOT software [33, 34]. NCI analysis revealed that this type of interaction was also present in the transition state of the coordination of azide **2a** either to Ru(β-Br$_4$TPP)CO (**3c**) or Ru(TMP)CO (**3f**). The large region of weak positive interactions can be visualized as the green surface between the azide phenyl ring and the catalyst's phenyl substituents showed in Fig. 4.

An energy barrier of 21.87 kcal/mol was found for the transition state involving Ru(3,5(CF$_3$)$_2$TPP)CO (**3d**)

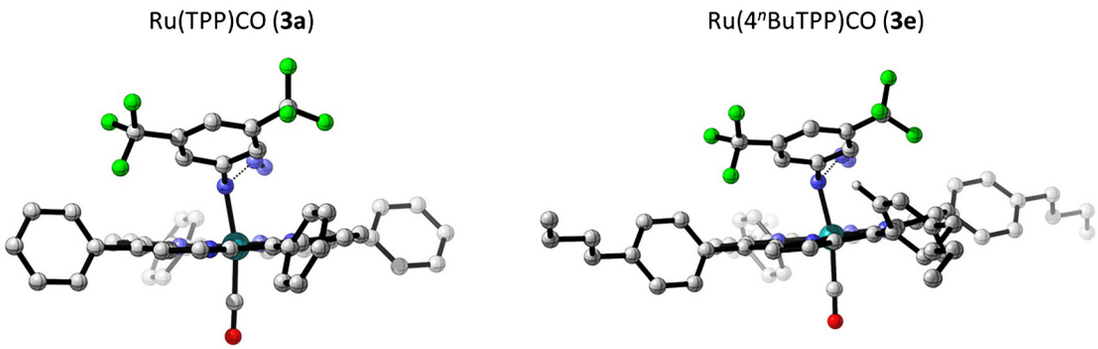

Fig. 3. Transition state structures related to the interaction of catalysts **3a** and **3e** with azide **2a**

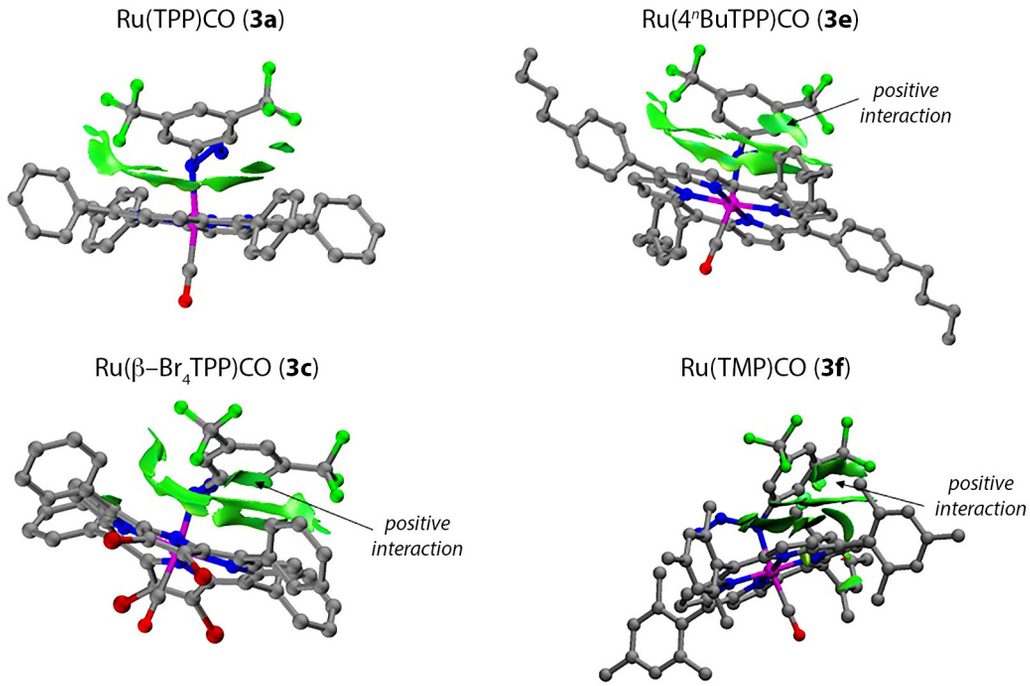

Fig. 4. NCIPLOT analysis performed in a selected cube (see Supporting information) using geometry calculated at the B3LYP/6-31G(d) Ru (SDD) level of theory for TSs related to catalysts **3a**, **3c, 3e** and **3f** with azide **2a**. Hydrogen atoms were omitted for clarity

Table 6. Ru–N distances of singlet **C(s)** and **C(t)** species relative to complexes **3a–3f**

Entry	Catalyst		Complex **C(s)** [Ru]–N distance, Å	Complex **C(t)** [Ru]–N distance, Å
1	Ru(TPP)CO	**3a**	1.889	1.978
2	Ru(OEP)CO	**3b**	1.882	1.970
3	Ru(β-Br_4TPP)CO	**3c**	1.891	1.985
4	Ru(3,5(CF_3)$_2$TPP)CO	**3d**	1.885	1.976
5	Ru(4^{n}Bu-TPP)CO	**3e**	1.887	1.985
6	Ru(TMP)CO	**3f**	1.881	1.956

catalyst. This highest energy barrier value was probably due to the presence of strong electron withdrawing CF_3 groups and the absence of π-staking stabilizations. This fact was confirmed by the lower yields obtained when this catalyst was employed in the aziridination process involving **2a** as the nitrene source (Table 3, entry 4).

The singlet → triplet spin crossing process of complexes **C** was also investigated by DFT calculations

(Table 5). As previously observed [28, 29], the high spin isomer was more stable than the singlet one. Lower value of $\Delta\Delta G^{\circ}$ $C_{(s)\rightarrow(t)}$ was observed when Ru(TPP)CO was used, where the difference between the singlet and triplet state was about 4.41 kcal/mol; the highest delta value (-7.62 kcal/mol) was obtained for Ru(TMP)CO (**3f**) catalyst.

Another important aspect was the increase of the $Ru–N_{imido}$ distance switching from the singlet species of complex **C(s)** to the corresponding **C(t)** complex in the triplet state (Table 6). In all the species investigated, the increase of the bond length was about +0.1 Å for the triplet state (Table 6), indicating its higher reactivity in the formation of diradical species **D**, in accordance with literature data [29].

EXPERIMENTAL

General

AQ: Closing bracket missing. Please check.

Unless otherwise specified, all the batch reactions were carried out under nitrogen atmosphere employing standard Schlenk techniques and magnetic stirring. Benzene and α-methylstyrene were dried over sodium and calcium hydride, respectively and stored under nitrogen. Ru(OEP)CO (**3b**) and Co(OEP) (**3g**) were commercially available and used as received. Compounds $3,5(CF_3)_2C_6H_3N_3$ (**2a**) [35], $4(NO_2)C_6H_4N_3$ (**2b**) [35], Ru(TPP)(CO) (**3a**) [36], Ru(β-Br_4TPP)CO (**3c**) [37], $Ru3,5(CF_3)_2$(TPP)CO (**3d**) [38], Ru(4″BuTPP)CO (**3e**) [36], Ru(TMP)CO (**3f**) [36], Co(TPP) (**3h**) [39], Co(TMOP) (**3i**) [40] were synthesized by methods reported in literature or using minor modifications of these methods. The purity of hydrocarbons and aryl azides employed was checked by GC-MS or ^{1}H NMR analyses. All the other starting materials were commercial products and used as received. NMR spectra were recorded at room temperature, unless otherwise specified, on a Bruker avance 300-DRX, operating at 300 MHz for ^{1}H, at 75 MHz for ^{13}C and at 282 MHz for ^{19}F. Chemical shifts (ppm) are reported relative to TMS. The ^{1}H NMR signals of the compounds described in the following have been attributed by COSY and NOESY techniques. Assignments of the resonance in ^{13}C NMR were made using the APT pulse sequence and HSQC and HMBC techniques. Infrared spectra were recorded on a Varian Scimitar FTS 1000 spectrophotometer. GC analysis were performed using Agilent 6850 single channel GC system. Mesoreactor was prepared using PTFE tubing for HPLC connections purchased from Supelco (1.58 mm outer diameter, 0.58 mm inner diameter, 1.89 m length, 500 µL effective volume) coiled in a bundle and immersed in an oil bath. A Chemix Fusion 100 syringe pump, equipped with one or two Hamilton gastight syringes, fed the reactant solutions through a T-junction into the above-mentioned PTFE tubing. The collected analytical data for *N*-(3,5-*bis*-(trifluoromethyl)phenyl)-2-phenylaziridine (**4a**) [41]; *N*-(4-nitrophenyl)-2-phenylaziridine (**4b**) [41] were in agreement with those reported in literature.

General procedure for catalytic reactions

***Method A* (*bach*).** In a typical run, the opportune catalyst (1.20×10^{-5} mol) the opportune azide (6.00×10^{-4} mol) and α-methylstyrene (2.50×10^{-3} mol) were added to benzene (25 mL) in a Schlenk flask. The reaction solution was refluxed by using a preheated oil bath. The consumption of the azide was monitored by IR spectroscopy measuring the characteristic azide absorbance in the region 2095–2130 cm^{-1}. The reaction was considered to be finished when the absorbance of the latter peak was below 0.03 (using a 0.5 mm thick cell). The solution was then concentrated to dryness and analyzed by ^{1}H NMR with 2,4-dinitrotoluene as the internal standard. All reaction times and products yields are reported in Tables 1 and 2.

***Method B* (*flow*).** In a typical experiment, syringe A was filled with a mixture obtained dissolving 0.02 eq (1.60×10^{-5} mol) of the opportune catalyst in 2.0 mL of the desired α-methylstyrene in order to have 0.008 M concentration of catalyst. The mixture was sonicated for 10 min and heated until a complete dissolution of the catalyst. Syringe B was filled with a mixture obtained dissolving 1.0 eq of the desired azide (8.00×10^{-4} mol) and 0.075 eq of biphenyl (6.00×10^{-5} mol, 9.2 mg) as the internal standard in 2.0 mL of α-methylstyrene in order to have 0.4 M concentration of azide (note: the concentrations of all reagents in the syringes were doubled with respect to the final concentration, to achieve the desired concentration after mixing). Syringes A and B were connected to a syringe pump and the reagents were pumped into PTFE mesoreactor at 120 °C through a T-junction at the flow rate of 8.333 µL/min (30 min as residence time). One reactor volume was discarded before starting sample collection in order to achieve steady-state conditions. Reaction outcome was collected into a vial cooled at -30 °C and directly analyzed by GC.

CONCLUSION

In conclusion, the addition of aryl azides to α-methylstyrene for the synthesis of *N*-aryl aziridines was successfully accomplished under batch and continuous-flow conditions, in the presence of a ruthenium and cobalt porphyrin-based catalysts. Generally speaking, higher yields were observed using ruthenium-based catalysts in a traditional batch process, but cobalt-based porphyrins presented higher chemical efficiency under flow conditions. Ru(TPP)CO (**3a**) and Ru(OEP)CO (**3b**) were the best catalysts for the aziridination of α-methylstyrene independent of the type of approach, while Co(OEP) (**3g**) was the best catalyst among the cobalt-based porphyrins investigated. This catalyst mediated the aziridination

process under solvent-free flow conditions in only 30 min at 120 °C using a 500 μL PTFE microreactor.

A preliminary DFT investigation about the catalytic effect of the substituent on the porphyrin ring in the aziridination process was also performed. This DFT study highlighted that the presence of electron donating substituents on the porphyrin ring facilitated the formation of the *mono*-imido [Ru](NAr)CO complex by dismissal of a N_2 molecule from the starting azide. In addition, electron rich ruthenium complexes showed also a higher stabilized triplet ground state which is considered the real active species in the aziridination process.

Acknowledgements

D.I and S. R. thanks Università degli studi di Milano for post-doc fellowships.

Supporting information

Supplementary material is available free of charge *via* the Internet at http://www.worldscinet.com/jpp/jpp.shtml.

REFERENCES

1. Yamaguchi J, Yamaguchi AD and Itami K. *Angew. Chem. Int. Ed.* 2012; **51**: 8960–9009.
2. Degennaro L, Trinchera P and Luisi R. *Chem. Rev.* 2014; **114**: 7881–7929.
3. Ohno H. *Chem. Rev.* 2014; **114**: 7784–7814.
4. Botuha C, Chemla F, Ferreira F and Pérez-Luna A. In *Aziridines in Natural Product Synthesis*, *Heterocycles in Natural Product Synthesis*, Majumdar KC and Chattopadhyay SK (Eds.) Wiley-VCH Verlag GmbH & Co. KGaA: 2011; pp. 1–39.
5. Singh GS, D'Hooghe M and De Kimpe N. *Chem. Rev.* 2007; **107**: 2080–2135.
6. *Aziridines and Epoxides in Organic Synthesis*, Yudin AK. (Ed.) Wiley-VCH Verlag GmbH & Co. KGaA: 2006; p. 492.
7. Fantauzzi S, Gallo E, Caselli A, Piangiolino C, Ragaini F, Re N and Cenini S. *Chemistry FIELD Full Journal Title:Chemistry* (*Weinheim an der Bergstrasse, Germany*) 2009; **15**: 1241–1251.
8. Pellissier H. *Adv. Synth. Catal.* 2014; **356**: 1899–1935.
9. Jung N and Bräse S. *Angew. Chem. Int. Ed.* 2012; **51**: 5538–5540.
10. Cramer SA and Jenkins DM. *J. Am. Chem. Soc.* 2011; **133**: 19342–19345.
11. Chang JWW, Ton TMU and Chan PWH. *Chem. Rec.* 2011; **11**: 331–357.
12. Fruit C, Robert-Peillard F, Bernardinelli G, Mueller P, Dodd RH and Dauban P. *Tetrahedron: Asymmetry* 2005; **16**: 3484–3487.
13. Evans DA, Faul MM and Bilodeau MT. *J. Org. Chem.* 1991; **56**: 6744.
14. Evans DA, Faul MA, Bilodeau MT, Andersson BA and Barnes DM. *J. Am. Chem. Soc.* 1993; **115**: 5328.
15. Evans DA, Bilodeau MT and Faul MM. *J. Am. Chem. Soc.* 1994; **116**: 2742.
16. Shin K, Kim H and Chang S. *Acc. Chem. Res.* 2015; **48**: 1040–1052.
17. Uchida T and Katsuki T. *Chem. Rec.* 2014; **14**: 117–129.
18. Intrieri D, Zardi P, Caselli A and Gallo E. *Chem. Commun.* 2014; **50**: 11440–11453.
19. Cenini S, Gallo E, Caselli A, Ragaini F, Fantauzzi S and Piangiolino C. *Coord. Chem. Rev.* 2006; **250**: 1234–1253.
20. Weber M, Yilmaz G and Wille G. *Chim. Oggi* 2011; **29**: 8–10.
21. Rossi S, Puglisi A, Benaglia M, Carminati DM, Intrieri D and Gallo E. *Catal. Sci. Technol.* 2016; **6**: 4700–4704.
22. Rossi S, Puglisi A, Intrieri D and Gallo E. *J. Flow Chem.* 2016; **6**: 234–239.
23. Fantauzzi S, Gallo E, Caselli A, Piangiolino C, Ragaini F and Cenini S. *Eur. J. Org. Chem.* 2007: 6053–6059.
24. Piangiolino C, Gallo E, Caselli A, Fantauzzi S, Ragaini F and Cenini S. *Eur. J. Org. Chem.* 2007: 743.
25. Fantauzzi S, Gallo E, Caselli A, Ragaini F, Macchi P, Casati N and Cenini S. *Organometallics* 2005; **24**: 4710–4713.
26. Goswami M, Lyaskovskyy V, Domingos SrR, Buma WJ, Woutersen S, Troeppner O, Ivanović-Burmazović I, Lu H, Cui X, Zhang XP, Reijerse EJ, DeBeer S, van Schooneveld MM, Pfaff FF, Ray K and de Bruin B. *J. Am. Chem. Soc.* 2015; **137**: 5468–5479.
27. Suarez AIO, Jiang H, Zhang XP and de Bruin B. *Dalton. Trans.* 2011; **40**: 5697–5705.
28. Zardi P, Pozzoli A, Ferretti F, Manca G, Mealli C and Gallo E. *Dalton. Trans.* 2015; **44**: 10479–10489.
29. Manca G, Gallo E, Intrieri D and Mealli C. *ACS Catal.* 2014: 823–832.
30. Banks JL, Beard HS, Cao Y, Cho AE, Damm W, Farid R, Felts AK, Halgren TA, Mainz DT, Maple JR, Murphy R, Philipp DM, Repasky MP, Zhang LY, Berne BJ, Friesner RA, Gallicchio E and Levy RM. *J. Comput. Chem.* 2005; **26**: 1752–1780.
31. The B97D functional was preferred to the standard B3LYP one for including dispersion forces. These can play an important role in systems where a delocalized metal-porphyrin planar unit weakly interacts with apically coordinated ligands. For more detail see Grimme S. *J. Chem. Phys.* 2006; **124**: 34108–35124.
32. Frisch MJ, Trucks GW, Schlegel HB, Scuseria GE, Robb MA, Cheeseman JR, Scalmani G, Barone V, Mennucci B, Petersson GA, Nakatsuji H, Caricato M, Li X, Hratchian HP, Izmaylov AF, Bloino J,

Zheng G, Sonnenberg JL, Hada M, Ehara M, Toyota K, Fukuda R, Hasegawa J, Ishida M, Nakajima T, Honda Y, Kitao O, Nakai H, Vreven T, Montgomery JA, Peralta JE, Ogliaro F, Bearpark M, Heyd JJ, Brothers E, Kudin KN, Staroverov VN, Keith T, Kobayashi R, Normand J, Raghavachari K, Rendell A, Burant JC, Iyengar SS, Tomasi J, Cossi M, Rega N, Millam JM, Klene M, Knox JE, Cross JB, Bakken V, Adamo C, Jaramillo J, Gomperts R, Stratmann RE, Yazyev O, Austin AJ, Cammi R, Pomelli C, Ochterski JW, Martin RL, Morokuma K, Zakrzewski VG, Voth GA, Salvador P, Dannenberg JJ, Dapprich S, Daniels AD, Farkas, Foresman JB, Ortiz JV, Cioslowski J and Fox DJ. Gaussian 09, Revision D.01. Wallingford CT, 2013.

33. Contreras-Garcia J, Johnson ER, Keinan S, Chaudret R, Piquemal JP, Beratan DN and Yang W. *J. Chem. Theory Comput.* 2011; **7**: 625–632.
34. Johnson ER, Keinan S, Mori-Sanchez P, Contreras-Garcia J, Cohen AJ and Yang W. *J. Am. Chem. Soc.* 2010; **132**: 6498–6506.
35. Tanno M, Sueyoshi S and Kamiya S. *Chem. Pharm. Bull.* 1982; **30**: 3125–3132.
36. Rillema DP, Nagle JK, Barringer LF and Meyer TJ. *J. Am. Chem. Soc*. 1981; **103**: 56–62.
37. Piangiolino C, Gallo E, Caselli A, Fantauzzi S, Ragaini F and Cenini S. *Eur. J. Org. Chem*. 2007; **2007**: 743–750.
38. Che CM, Zhang JL, Zhang R, Huang JS, Lai TS, Tsui WM, Zhou XG, Zhou ZY, Zhu N and Chang CK. *Chemistry* 2005; **11**: 7040–7053.
39. Adler AD, Longo FR and Varadi V. *Inorg. Synth*. 1976; **16**: 213–220.
40. Polam JR, Shokhireva TK, Raffii K, Simonis U and Walker FA. *Inorg. Chim. Acta* 1997; **263**: 109–117.
41. Fantauzzi S, Gallo E, Caselli A, Piangiolino C, Ragaini F and Cenini S. *Eur. J. Org. Chem.* 2007; **2007**: 6053–6059.